Performance of Waveband MUX/DEMUX Using Concatenated AWGs

S. Kakehashi, *Student Member, IEEE*, H. Hasegawa, *Member, IEEE*, K. Sato, *Fellow, IEEE*, O. Moriwaki, *Member, IEEE*, S. Kamei, Y. Jinnouchi, and M. Okuno, *Member, IEEE*

***Abstract*—Recently, we proposed a new waveband multi/demultiplexer that uses two concatenated arrayed-waveguide gratings. We fabricate the device using silica planar lightwave circuit technology and experimentally confirm its feasibility. The device was designed to accommodate 40 100-GHz-spaced C-band channels on the ITU-T grid and six input fibers simultaneously, that is, one chip can support 240 channels.**

***Index Terms*—Arrayed-waveguide grating (AWG), planar lightwave circuit (PLC), waveband (WB) multi/demultiplexer (MUX/DEMUX).**

I. Introduction

BROADBAND access is being rapidly adopted throughout the world and, as a result, traffic is continually increasing. Further traffic expansion will occur in the near future with the introduction of new broadband services including IP video and HDTV, which will warrant the introduction of the hierarchical optical path cross-connect (HOXC) [1]. Hierarchical optical paths have been shown to decrease the total cost of optical cross-connects [2]. One key component in realizing the HOXC is the waveband [(WB) a group of wavelength channels in dense wavelength-division multiplexing] multi/demultiplexer (MUX/DEMUX). A thin-film filter has been reported that offers 8-skip-0 band operation supporting a total of 32 channels at 100-GHz spacing [3]. Unfortunately, it requires 409 layers [3] so the manufacturing challenge is significant. Furthermore, it demonstrates strong nonlinear dispersion at the band edges. Other band filters based on arrayed-waveguide gratings (AWGs) have been reported. They realize an 8-skip-0 band configuration with a total of 40 channels and 100-GHz spacing [4]. It uses two AWGs with 110 input–output ports and 127 input–output ports; note that the length of each waveguide connecting the two AWGs must be equal.

A more recent proposal [5] uses concatenated cyclic AWGs to realize the WB MUX/DEMUX. The key to the WB MUX/DEMUX is that it retains multi/demultiplexing granularity at the individual wavelength channel level while

Manuscript received February 5, 2007; revised May 10, 2007. This work was supported in part by JST.

S. Kakehashi, H. Hasegawa, and K. Sato are with Nagoya University, Ghikusa-ku, Nagoya 464-8603, Japan (e-mail: s_kakeha@echo.nuee.nagoya-u.ac.jp).

O. Moriwaki and S. Kamei are with NTT Photonics Laboratories, NTT Corporation, Atsugi, Kanagawa 243-0198, Japan.

Y. Jinnouchi and M. Okuno are with NTT Electronics, NTT Corporation, Naka, Ibaraki 311-0122, Japan.

Color versions of one or more of the figures in this letter are available online at http://ieeexplore.ieee.org.

Digital Object Identifier 10.1109/LPT.2007.901602

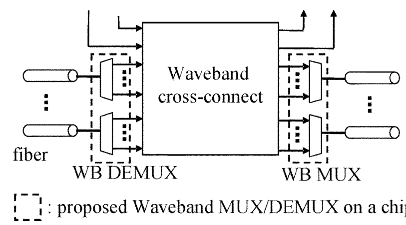

Fig. 1. Configuration of node with multiple input fibers.

outputting WBs at different ports. The AWGs are thus conventional ones with wavelength channel resolution on the International Telecommunication Union (ITU-T) grid. The length of each waveguide/fiber connecting the two AWGs is arbitrary and, hence, the device can be smaller due to the inherent layout flexibility. Indeed, the fabricated device adopted a folded layout of two AWGs, which can reduce chip size (and, hence, necessary substrate size). The salient feature of the WB MUX/DEMUX is that it can accommodate multiple input fibers simultaneously and demultiplex each band to different output ports, which makes it very effective in reducing the cost and size of WBXC (see Fig. 1). In [5], possible arrangements of two-AWG concatenation were elucidated. Connection patterns that eliminate all waveguide crossing, which suits monolithic realization, were demonstrated, and those that maximize MUX/DEMUX port utilization efficiency were also provided. In this letter, we generalize and formulate the connection arrangements. We then demonstrate fabrication of the device using silica planar lightwave circuit (PLC) technology on a chip. Measured performance of the device is introduced and the crosstalk characteristic is also discussed. A preliminary fabrication report was presented at an international conference [6].

II. Formulation of Port Connections of Two AWGs

There are two ways of concatenating two AWGs: the continuous WB arrangement and the dispersive (interleaved) WB arrangement [5]. The former can eliminate all waveguide crossings; while the latter cannot match this attribute, it can maximize MUX/DEMUX port utilization efficiency [5]. The continuous WB arrangement is, therefore, more suitable for monolithic fabrication. Because of space limits, we show below only the results of the continuous WB arrangement.

In a cyclic AWG with M input and M output ports, the output port number (# output port) for each pair of wavelength number (# wavelength) and input port number (# input port) is determined by

$$\#\,\text{output port} = \{\#\,\text{wavelength} - \#\,\text{input port}\}_{\text{mod}M} + 1. \tag{1}$$

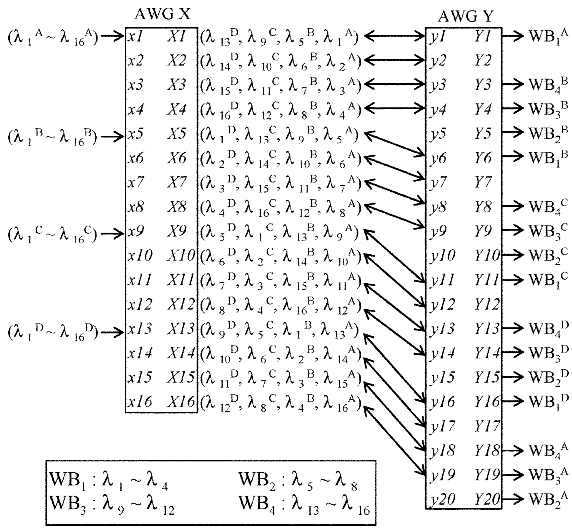

Fig. 2. WB MUX/DEMUX utilizing cyclic AWGs.

Here, cyclic means that the free-spectral range (FSR) of the $M \times M$ AWG corresponds to the width that covers M channels.

Even for the continuous WB arrangements, there are several possible waveguide connection arrangements between AWG X and Y and various realization strategies using different sets of AWGs. In this letter, only the most fundamental ones are discussed hereafter; variations that introduce additional AWG ports, which decrease port utilization, are not considered. Let M be the total number of wavelength paths per fiber, B the number of WBs per fiber, and D the number of wavelength paths per WB. Hence, the product of B and D equals M. λ_1^A and WB_1^A represent wavelength path 1 in Fiber A and WB 1 in Fiber A, respectively. The input side AWG is denoted as AWG X and the output side AWG as AWG Y; $xi(yi)$ represents the number i input port of AWG X (Y), and $Xi(Yi)$ represents the number i output port of AWG X (Y) (see Fig. 2).

Let the kth WB WB_k $(k = 1, \sim, B)$ accommodate D wavelength paths $\lambda_{(k-1)D+1}, \sim, \lambda_{kD}$. Suppose that AWG X and AWG Y have sizes of $M \times M$ and $N \times N (N \geq M + B)$, respectively. In this case, a proposed WB MUX/DEMUX is realized by the following connections between # $\mathrm{X_{out}}$ of AWG X and # $\mathrm{y_{in}}$ of AWG Y

$$\# y_{\mathrm{in}} = \# \mathrm{X_{out}} + j\left[(\# \mathrm{X_{out}} - 1)/D\right] + i$$
$$(1 \leq \# \mathrm{X_{out}} = M, 1 \leq \# y_{\mathrm{in}} \leq N) \quad (2)$$

where $[z]$ is the largest integer such that $[z] \leq z$, and i, j are integers satisfying the following relations:

$$i + j(B-1) + DB \leq N, \qquad i \geq 0,\ j \geq 1. \quad (3)$$

Input fiber connection ports to AWG X can be determined as

$$\# x_{\mathrm{in}} = 1 + sD \quad (1 \leq x_{\mathrm{in}} \leq M) \quad (4)$$

where s is an integer satisfying $0 \leq s \leq B - 1$. Please note that multiple input fibers that satisfy (4) can be accommodated. With AWG X, the size of which is larger than M, it is possible to create a WB MUX/DEMUX that can multi/demultiplex WBs, however, port usage is degraded. Fig. 2 shows an example of our proposed MUX/DEMUX, where M, B, D, and N equal 16, 4, 4, and 20, respectively. Parameters i and j are set at 0 and 1, respectively. It should be noted that the device can accommodate four input fibers simultaneously and eliminate all waveguide crossings between the two AWGs. The formulas for dispersive (interleaved) WB arrangement can be derived similarly; they are not shown here because of the space limitation.

One problem with fabricating large cyclic AWGs is the difficulty of precisely aligning the center of each channel frequency on the ITU-T grid at each output port. The use of wide FSR AWG (conventional AWG) can relax this problem, but it lowers port utilization efficiency. In order to verify the basic performance of our proposed device, we fabricated a WB MUX/DEMUX utilizing wide FSR AWGs (same FSR for the two AWGs).

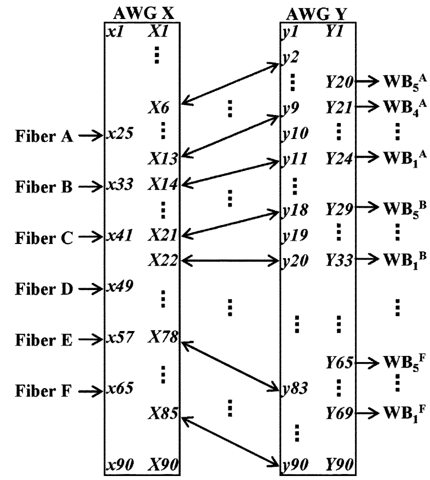

Fig. 3. Fabricated WB MUX/DEMUX utilizing wide FSR AWGs.

Fig. 3 depicts the connection arrangement of the fabricated WB MUX/DEMUX. It used two AWGs, X and Y; each has 90 input and 90 output ports. Eighty output waveguides out of the 90 were used to connect two AWGs. The relation among output port number, wavelength number, and input port number is given by (5)

$$\#\,\text{output port} = \#\,\text{wavelength} - \#\,\text{input port} + 70. \quad (5)$$

When 40 channels are to be demultiplexed into five WBs, each of which consists of eight wavelength channels, the proposed WB MUX/DEMUX is realized by the following connections between # $\mathrm{X_{out}}$ of AWG X and # $\mathrm{y_{in}}$ of AWG Y

$$\# y_{\mathrm{in}} = \# \mathrm{X_{out}} + \left[(\# \mathrm{X_{out}} - 6)/8\right] - 4. \quad (6)$$

The connection arrangement is shown in Fig. 3. The device can support six input fibers simultaneously, each carrying 40 wavelength channels. Accordingly, the device consists of six input fiber ports and 30 WB output ports.

III. Experiments

The device was designed to accommodate 40 100-GHz-spaced channels ($191.8 + 0.1 \times n[\mathrm{THz}]$; $n = 0 \sim 39$) on the ITU-T grid. The device was fabricated using PLC technology on one chip; chip size was 3 × 7 cm as shown in Fig. 4. The left and right images show the chip and the layout, respectively. The waveguide cross-section dimensions and index contrast of

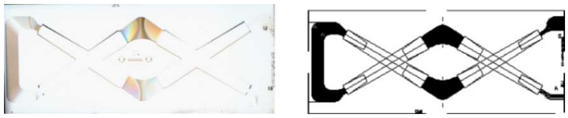

Fig. 4. Fabricated WB MUX/DEMUX chip (left) and the layout (right).

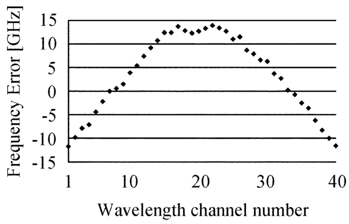

Fig. 5. Frequency differences between passband peak and ITU-T grid.

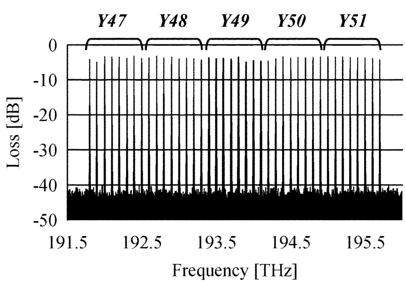

Fig. 6. Output channel spectra at output ports $Y47, Y48, Y49, Y50,$ and $Y51$, when six input fibers are connected to ports of $x25$, $x33$, $x41$, $x49$, $x57$, and $x65$.

the chip were 4.5 μm $\times$ 4.5 μm and 1.5%, respectively. The grating order of the AWG X and Y was 16.

One of the important design issues is aligning the output passband peaks on the ITU-T grid. Fig. 5 shows measured frequency differences between passband peak and ITU-T grid from λ_1 to λ_{40} when input Fiber A is connected to port x25. The maximum difference was $+/-15$ GHz, which almost equals the design value. Frequency differences for other input fibers are almost the same as those for Fiber A.

Fig. 6 shows examples of output channel spectra of WBs at output ports $Y47$, $Y48$, $Y49$, $Y50$, and $Y51$, when six fibers were connected to ports $x25$, $x33$, $x41$, $x49$, $x57$, and $x65$ (each fiber carries 40-channels on the ITU-T grid). This figure shows that the device retains multi/demultiplexing granularity at the individual wavelength channel level while outputting WBs at different ports. Outputs from other WB output ports Yij were also measured and the routing capability of the fabricated device was confirmed to be accurate. The measured average fiber-to-fiber insertion loss was 3.83 dB, respectively. The worst and average coherent crosstalk was less than -34.0 and -39.5 dB, respectively, when six input fibers were connected simultaneously. The adjacent band crosstalk is relatively high compared to the coherent crosstalk levels at the output ports. This is because the output waveguides are relatively closely spaced and as a result, the adjacent band leaks from the neighboring output ports. Fig. 7 shows output channel spectra at port $Y50$ when an input fiber was connected to ports $x49$; the worst adjacent crosstalk at the output port $Y50$ was about -20 dB. This adjacent crosstalk is, however, eliminated by passing the signal through the WB MUX connected to the output fiber (see Fig. 1). For example, when an

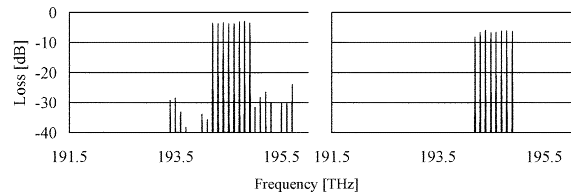

Fig. 7. Left is output channel spectra at output port $Y50$, when an input fiber is connected to port $x49$. Right is output channel spectra after traversing the set of WB DEMUX (AWG X-Y) and WB MUX (AWG Y-X). Output channel spectra at WB MUX output port $x41$, when an input fiber is connected to WB DEMUX port $x49$ and the output port $Y50$ is connected to WB MUX input port $Y41$.

input fiber was connected to port $x49$ and WB_2^D and the adjacent crosstalk from output port $Y50$ were switched by WB cross-connect switch (see Fig. 1) and fed to input port $Y41$ of WB MUX (the input and output directions in Fig. 3 are opposite to implement DEMUX and MUX) after cross-connection, the worst adjacent crosstalk at output port $x41$, to which WB WB_2^D is routed, was less than -30 dB, as shown in Fig. 7 (output channel spectra at port $x49$ through WB MUX). This is because all the adjacent crosstalk is output at the ports other than those used to connect output fibers [this can be easily proven from (5)]. Hence, the crosstalk signals experience a large additional attenuation, at least 20 dB. For example, in the case of Fig. 3, the worst adjacent crosstalk in Fig. 7 is delivered to and output at output port $x40$ [see (5)] after passing through the WB MUX. Furthermore, because the WB MUX output ports connected to six fibers do not neighbor each other, adjacent crosstalk is suppressed to the level that causes no deterioration in signal quality.

IV. Conclusion

We introduced formulations for connecting waveguides in a recently proposed WB MUX/DEMUX realized by connecting two AWGs. The device, which supports six input fibers each carrying 40 C-band channels (eight channels $\times$ five WBs) on the 100-GHz ITU-T grid, was successfully fabricated using silica PLC technology on a chip. The average fiber-to-fiber insertion loss was 3.83 dB. This device is very useful in creating cost-effective and compact WB cross-connects.

References

[1] L. Noirie, C. Blaizot, and E. Dotaro, "Multi-granularity optical cross-connect," in *Proc. ECOC*, Oct. 2000, vol. 3, pp. 269–270.
[2] I. Yagyu, H. Hasegawa, and K. Sato, "An efficient hierarchical optical path network design algorithm based on a traffic demand expression in a cartesian product space," in *Proc. ECOC*, Sep. 2006, vol. 2, pp. 113–114.
[3] G. J. Ockenfuss, N. A. O'Brien, and E. Williams, "Ultra-low stress coating process: An enabling technology for extreme performance thin film interference filters," in *Proc. OFC*, Mar. 2002, Postdeadline paper PDFA8.
[4] S. Chandrasekhar, C. R. Doerr, and L. L. Buhl, "Flexible waveband optical networking without guard bands using novel 8-skip-0 banding filters," *IEEE Photon. Technol. Lett.*, vol. 17, no. 3, pp. 579–581, Mar. 2005.
[5] S. Kakehashi, H. Hasegawa, K. Sato, and O. Moriwaki, "Waveband MUX/DEMUX using concatenated arrayd-waveguide gratings," in *Proc. ECOC*, Sep. 2006, vol. 3, pp. 233–234.
[6] S. Kakehashi, H. Hasegawa, K. Sato, O. Moriwaki, S. Kamei, Y. Jinnouchi, and M. Okuno, "Waveband MUX/DEMUX using concatenated AWGs—Formulation of waveguide connection and fabrication," in *Proc. OFC*, Mar. 2007, Paper JThA94.